Dye-Modified Nanochannel Materials for Photoelectronic and Optical Devices
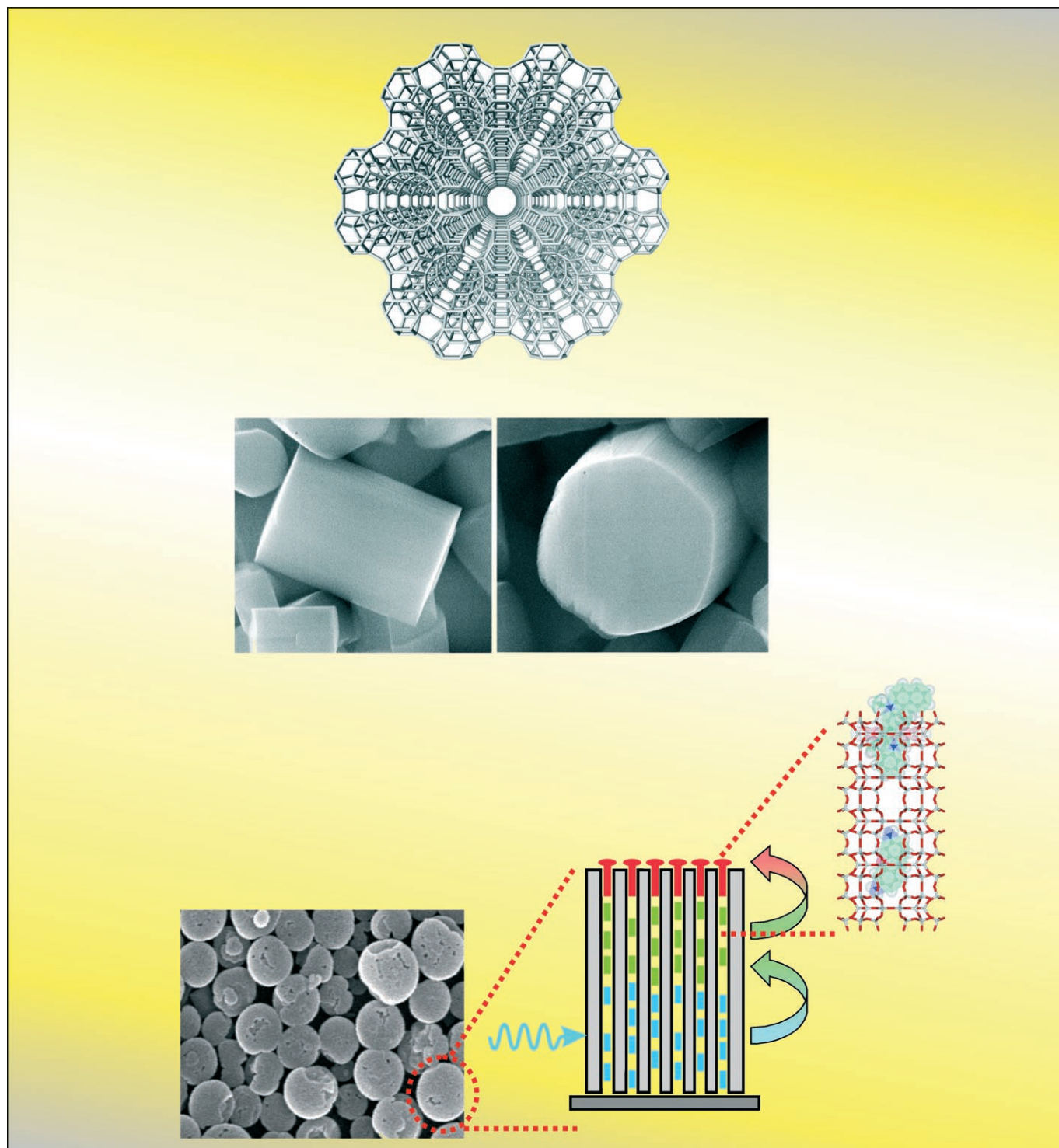
Gion Calzaferri,*[a] Huanrong Li,*[b] and Dominik Brühwiler*[c]

Abstract: Artificial photonic antenna systems have been realised by incorporating organic dyes into zeolite L. The size and aspect ratio of the cylindrically shaped zeolite crystals can be tuned over a wide range, adding to the versatility of this host material. A 600 nm sized crystal, for example, consists of about 96 000 one-dimensional channels oriented parallel to the cylinder axis. Geometrical constraints imposed by the host structure lead to supramolecular organisation of the guests, allowing high concentrations of non- or only very weakly interacting dye molecules. A special twist is added to these systems by plugging the channel openings with a second type of fluorescent dye, a so-called stopcock molecule. The two types of molecules are precisely tuned to each other; the stopcocks are able to accept excitation energy from the dyes in the channels, but cannot pass it back. The supramolecular organisation of dyes in the zeolite channels corresponds to a first stage of organisation, allowing light-harvesting within the volume of a cylindrical crystal and radiationless energy transport to either the cylinder ends or centre. The second stage of organisation represents the coupling to an external acceptor or donor stopcock fluorophore at the channel entrances, which can then trap or inject electronic excitation energy. The third stage of organisation is realised by interfacing the material to an external device through a stopcock intermediate. We observed that electronic-excitation-energy transfer in dye–zeolite L materials occurs mainly along the channel axis and we have shown that macroscopically organised materials can be prepared. The new materials offer unique possibilities as building blocks for optical, electro-optical and sensing devices.

Keywords: dyes/pigments · FRET (fluorescence resonant energy transfer) · host–guest systems · luminescence · supramolecular chemistry · zeolites

[a] Prof. Dr. G. Calzaferri
Department of Chemistry and Biochemistry
University of Bern, Freiestrasse 3, 3012 Bern (Switzerland)
Fax: (+41) 31-63-13-994
E-mail: gion.calzaferri@iac.unibe.ch

[b] Prof. Dr. H. Li
School of Chemical Engineering
Hebei University of Technology, Tianjin, 300130 (China)
Fax: (+86) 222-6564294
E-mail: lihuanrong@hebut.edu.cn

[c] Dr. D. Brühwiler
Institute of Inorganic Chemistry
University of Zürich
Winterthurerstrasse 190, 8057 Zürich (Switzerland)
Fax: (+41) 44-63-568-02
E-mail: bruehwi@aci.uzh.ch

Introduction

One-dimensional channel materials are very attractive hosts for supramolecular organisation of guests.[1,2] They are often, at least conceptually, the simplest possible choice for obtaining a specific organisational pattern. A large variety of systems have been realised by using zeolite L as a host and luminescent dye molecules as guests.[2–4] Zeolite L consists of strictly parallel channels arranged in a hexagonal framework as shown in Figure 1. Its stoichiometry is $[M]^+_9$-$[(AlO_2)_9(SiO_2)_{27}] \cdot n\,H_2O$, in which M^+ are monovalent ions compensating the negative charge resulting from the aluminium atoms and n is 21 in fully hydrated materials, and 16 at about 22 % relative humidity.[5] Zeolite L currently seems to be the only nanochannel material that can be synthesised in a size range starting from about 30 nm up to a few thousand nm and with different aspect ratios from disc-shaped to elongated crystals.[6] In a theoretical study, we examined cylinders containing donor and acceptor molecules in an arrangement as shown in Figure 1F.[7] The donors are represented in green and the acceptors in red. The donor that has been excited by absorbing an incident photon transfers its electronic excitation radiationlessly by means of Förster resonance energy transfer (FRET) to an unexcited neighbour.[8] After a series of such steps, the electronic excitation reaches a luminescent trap (acceptor molecule) and is then released as fluorescence. The acceptors are thought to mimic the "entrance of the reaction centre" of the natural antenna. The dimensions given in Figure 1F correspond to the pore opening and the distance between the centres of two channels in zeolite L. The largest energy-transfer rate constant is observed if the electronic transition dipole moments (ETDM) are oriented parallel to the channel axis. Quasi one-dimensional energy transfer, an important requirement for an efficient light-harvesting material, was observed, and the first unidirectional antenna system realised on a macroscopic scale has been reported.[9,10] In the following, we will present selected features of these new materials specifically concerning their unique possibilities as building blocks for optical, electro-optical and sensing devices. Table 1 shows the structure of the dyes that were used as guest molecules for the materials discussed in this article.

Organisation

Antenna systems are supramolecular arrangements in which electronic excitation of molecules occurs in a given volume and in which the electronic excitation energy is then transported by near-field interactions (FRET) to a well-defined location. Sequential insertion of dyes into zeolite L channels is an excellent concept for preparing such systems.[11] Communication of the dyes in the channels with the outside world is established by stopcocks, consisting in principle of a label, a spacer and a head as shown in Figure 2.[12] The

Figure 1. Host material and schematic representations of an artificial photonic antenna. A) Zeolite L framework projected along the *c* axis. The lines represent oxygen bridges between Si and Si/Al. B) Van der Waals representation with a dye molecule (Th$^+$) entering one of the channels. C) Schematic representation of the top view of some channels. D) SEM image showing a side and top view of zeolite L crystals. The length of the crystal on the left is around 950 nm, whereas the diameter of the crystal on the right is around 850 nm. E) Side view of a channel. The opening of the channel is 0.71 nm. The largest inner diameter is 1.26 nm, the length of a unit cell is 0.75 nm, and the centre to centre distance between two channels is 1.84 nm. The double arrow indicates an example of the orientation of the ETDM $\mu_{S_1 \leftarrow S_0}$ of a dye. F) Schematic representation of an artificial antenna. The chromophores are embedded in the channels of the host. The green dyes act as donor molecules, which absorb the incoming light and transport the electronic excitation energy by FRET to the red acceptors. The process can be analysed by measuring the emission of the red acceptors and comparing it with that of the donors. G) Unidirectional antenna system oriented on a macroscopic scale. The SEM image on the left shows a monolayer of standing zeolite L crystals of an average diameter of about 900 nm. The adjacent schematic illustrates a standing zeolite crystal loaded with two types of dye and modified with stopcock molecules at the channel ends. The magnification shows a channel with dye and stopcock.

Table 1. Dyes and abbreviations

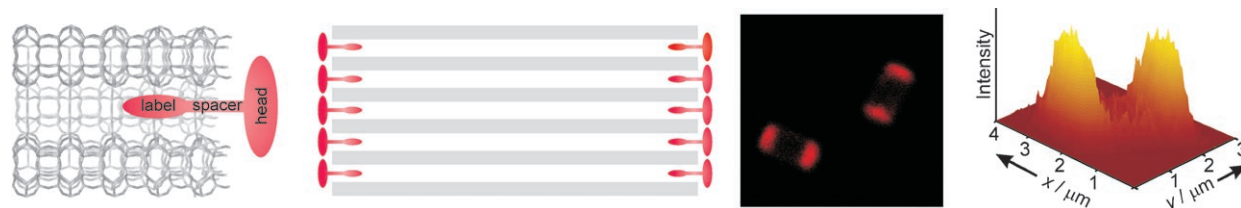| Abbreviation	Structural formula	Abbreviation	Structural formula
Th$^+$		DMPOPOP	
Ox$^+$		SG5	
PC21$^+$		PR 149 DXP	
ATTO-610		BNCO	

Figure 2. Stopcock principle. Left: A channel entrance with a schematically represented stopcock molecule. Middle: A zeolite crystal modified with stopcock molecules at the channel entrances. Right: Confocal fluorescence microscopy images of ATTO-610-zeolite L crystals. The two images indicate that only the base of the crystal is modified with ATTO-610.

heads of these molecules are too large to enter the channels. Luminescent stopcocks can be used to extract or inject electronic excitation energy from or into the zeolite L crystals by means of FRET. Stopcocks can also prevent penetration of small molecules, such as oxygen and water, or hinder encapsulated molecules, clusters, and cations from leaving the channels. Depending on the type, stopcocks can be bound either by physisorption, by electrostatic interaction, by covalent bonding or by a combination of electrostatic and covalent bonding. A versatile method for covalently attaching stopcock molecules to the channel entrances is by first grafting an amino group, which can then be treated with any amino-reactive molecule, as illustrated in Scheme 1.[13–15] A selection of stopcocks successfully used so far can be found in ref. [4].

The best way to find out if and where the stopcock molecules are attached to a crystal is fluorescence microscopy—if possible in confocal mode—on crystals of different size. Figure 2 (right) shows as an example ATTO-610 covalently attached to the channel entrances of a zeolite L crystal. The red luminescence on both crystal bases originates from the attached ATTO-610. Stopcock-plugged antennae are dye-loaded zeolite crystals in which either the donors or the acceptors are stopcock molecules.

Figure 3 presents a selection of materials that have been successfully prepared, fulfilling the criteria of different stages of supramolecular organisation. The length of the zeolite L crystals that have been used ranges from about 30 nm up to a few thousand nm. The channel walls are shown as grey bars, as in Figure 2, the dye molecules in the channels are shown as coloured rectangles and the stopcocks are drawn in a similar way as in Figure 2. Figure 3A shows antenna materials that can be obtained by consecutive insertion of different dye molecules, either from gas phase or from solution, depending on the type of dye and the desired

result. Stopcock-plugged antenna materials are obtained by modifying the channel entrances with specific stopcock molecules. The excitation energy from the dyes in the channels is transported by means of FRET to the molecules located at the entrances, which optionally can be stopcocks. Figure 3B illustrates a bidirectional dye1/dye2/zeolite L antenna; blue-emitting donors transfer electronic excitation energy to red-emitting acceptors at the ends of the cylindrical crystal. A 2 μm long crystal containing DMPOPOP in the middle part and Ox^+ at both ends as seen in a fluorescence microscope is shown. Since the ETDM of DMPOPOP is parallel to the c axis and that of Ox^+ is oriented at 73°,[16] the two fluorescence microscopy images were conveniently obtained by means of an adequately oriented polarizer. The orientation and the arrangement of molecules depend on their size and shape. We are mainly interested in dyes that are so large that they cannot pass each other in the channels, as this enables us to obtain the desired organisational patterns. Some of these dyes have a shape that prevents close enough contact for significant J-aggregate coupling, while others can be packed so tightly that such coupling is to be expected.[17,18] This is illustrated in Figure 3C, in which we show a simplified view of different orientations and two arrangements of molecules in the channels.[19] Four representative orientations of molecules and their ETDM, indicated by the double arrow, are illustrated. The large molecules shown in the middle align parallel to the channel axis and feature no electronic interaction because of their size and shape. The orientation of large molecules that align parallel to the channel axis and which have some electronic interaction, because of their shape, is shown at the bottom. Observation of J-aggregate coupling of dyes in the channels of zeolite L has recently been reported.[4,20]

Hierarchically organised structures, featuring successive ordering from the molecular to the macroscopic scale are
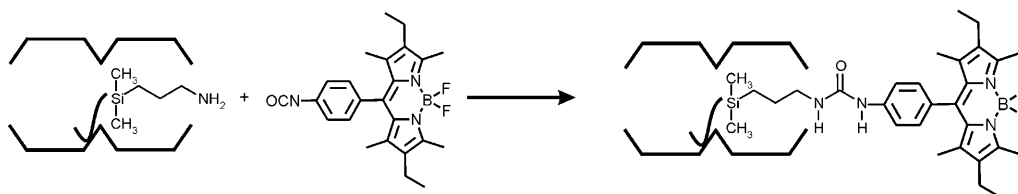
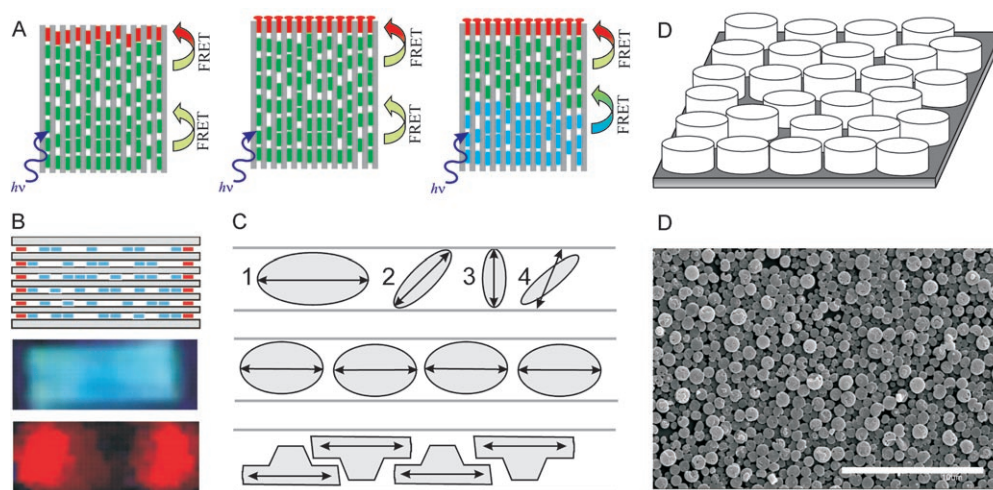Scheme 1. Covalent binding of BNCO to the channel entrance of zeolite L.

Figure 3. Materials fulfilling the criteria of different stages of supramolecular organisation. A) Antenna materials and stopcock-plugged antenna materials. The excitation energy from the dyes in the channels (green and blue rectangles) is transported by FRET to the molecules (red) located at the entrances. B) Dye-loaded zeolite L antenna; blue-emitting donors in the channels transfer electronic excitation energy to red-emitting acceptors at the left and right of the cylindrical crystal. Fluorescence microscopy images of a 2 μm long crystal containing DMPOPOP in the middle part and Ox⁺ at both ends. C) Simplified view of different orientations and two arrangements of molecules in the channels. Top: four representative orientations of molecules and their ETDM, indicated by the double arrow. Middle: orientation of large molecules which align parallel to the channel axis and which have no electronic interaction because of their size and shape. Bottom: orientation of large molecules which align parallel to the channel axis and which have some electronic interaction because of their shape. D) Oriented monolayers of standing zeolite L crystals on a substrate. Top: schematic view. Bottom: SEM image of a monolayer on glass. The length of the scale bar is 10 μm.

subject of great interest due to the relationship between the molecular arrangements and the macroscopic properties. A possibility for achieving a higher level of organisation is the controlled assembly of the zeolite crystals into oriented structures in which the cylindrically shaped zeolite L crystals are standing on their base surfaces. As a consequence, alignment of a large number of one-dimensional channels is obtained. Figure 3D shows a schematic view and an SEM image of a monolayer on glass.[10] An underlying principle that has to be considered when preparing such a material is that the interaction between the base of the zeolite L crystals and the substrate must be stronger or much stronger than the interaction with the coat and any base–base or base–coat interaction among the zeolite crystals themselves. Working with an excess of crystals, fixing them in the right way to the substrate and washing away the excess material generally leads to the desired assembly, provided that the starting material features a narrow particle size distribution and good morphology. Subsequent insertion of dye molecules into the channels and addition of stopcocks is only feasible if the channels are not blocked or damaged during the preparation of the monolayer.[10]

The stopcock principle outlined above enables communication of dyes in the channels with external species such as a molecule, a polymer matrix, a semiconductor, a quantum-sized particle, a molecular or nanomagnet, and a biochemical or a biological object. This principle is illustrated in Figures 1G and 3A. Here, we describe, as an example, an energy-transfer material containing gas-phase-deposited solvent green (SG5) in the channels of zeolite L and the bodipy dye BNCO[21] attached to the channel entrances ac-

cording to a procedure described in reference [13] (Scheme 1). Figure 4 shows the result of an energy-transfer experiment performed with this material. The fluorescence spectrum of SG5 and the excitation spectrum of BNCO
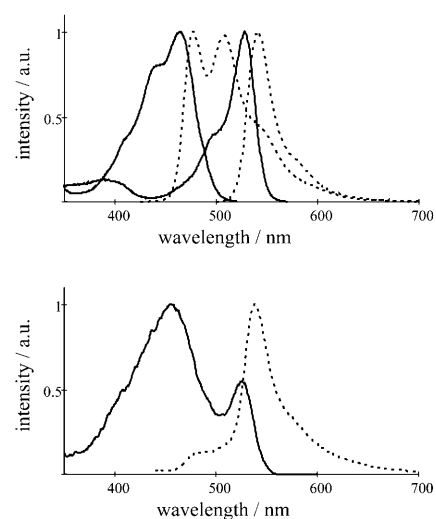

Figure 4. Energy-transfer experiment. Top: Excitation (solid) and emission (dashed) spectra of SG5 in ethanol and of BNCO in CH_2Cl_2. The fluorescence spectrum of SG5 was measured upon excitation at 410 nm; the excitation spectrum was recorded at fixed fluorescence wavelength of 560 nm. The emission spectrum of BNCO was measured upon excitation at 460 nm; the excitation spectrum was recorded at fixed fluorescence wavelength of 600 nm. Bottom: Excitation (solid) and emission (dashed) spectra of BNCO,SG5-zeolite L. The emission spectrum was recorded upon selective excitation of SG5 at 430 nm. The excitation spectrum was recorded at fixed fluorescence wavelength of 640 nm.

shown on the left indicate a large spectral overlap essential for efficient FRET. The excitation and the fluorescence spectrum of the bidirectional BNCO/SG5/zeolite L antenna are shown on the right. Energy transfer from SG5 to the bodipy dye attached to both sides of the cylindrically shaped crystals is nearly quantitative. When handling SG5 care must be taken in order to avoid hydrolysis and subsequent alteration of its photophysical properties.[22] Similar experiments have also been made on monolayers of standing zeolite L crystals corresponding to the arrangement shown in Figure 1G.[10]

The Förster energy-transfer rate constant k_{EnT} [Eq. (1)] has been derived based on dipole–dipole interactions between the ETDM of donor and acceptor.[8] J-aggregate interaction leading to exciton splitting β_c [Eq. (2)] is based on a similar type of dipole–dipole interaction.[17,18]

$$k_{EnT} = TF \frac{\kappa_{D*A}^2}{R_{D*A}^6} \frac{\phi_{D*}}{\tau_{D*}} J_{D*A} \frac{1}{n^4} \qquad (1)$$

$$\beta_c = AD \frac{\kappa_{A*A}}{R^3} \frac{f}{\Delta E} \frac{1}{n^2} \qquad (2)$$

In Equation (1) R_{D*A} is the distance between the electronically excited donor D* and the acceptor A, τ_{D*} is the decay time, ϕ_{D*} is the luminescence quantum yield of the donor, both in absence of energy transfer, n is the refractive index of the environment, J_{D*A} is the spectral overlap between the luminescence spectrum of the donor and the absorption spectrum of the acceptor and κ_{D*A}^2 is the orientation factor describing the dependence of the energy-transfer rate constant on the relative orientation of the ETDM of $D*$ and A. It is convenient to define the Theodor Förster constant TF, which is equal to 8.785×10^{-25} mol, if the spectral overlap integral J_{D*A} is expressed in $cm^3 M^{-1}$, the distance R_{D*A} in Å, the decay time τ_{D*} in ns, and the rate constant k_{EnT} in ns^{-1}.

The J-aggregate coupling strength β_c between two molecules $(A*\cdots A)\leftrightarrow(A\cdots A*)$, in which A* denotes an electronically excited molecule A, and the splitting of the levels depend on the relative orientation of the ETDM κ_{A*A}, the distance R and the refractive index n of the medium. AD is a constant that takes a value of 1.615×10^{-18} $m^2 cm^{-1}$ if β_c is expressed in cm^{-1}.

The coupling is largest for in-line orientation. It leads to J-coupling, while H-coupling occurs at essentially parallel arrangement.[18] The validity of both equations depends on the condition that the distance between the ETDM of two involved molecules is large with respect to the length of the ETDM. It can be shown that the length $l_{\mu*}$ of the ETDM can be expressed as Equation (3), in which the constant is equal to 3.036×10^{-6} $cm^{0.5}$ and ΔE is the $S_1 \leftarrow S_0$ electronic excitation energy in cm^{-1}

$$l_{\mu*} = const \sqrt{(f/\Delta E)} \qquad (3)$$

From this equation we find, as an example, the length of the ETDM of an organic molecule with an oscillator

strength of $f = 1$ absorbing at 500 nm to be 0.215 nm. This means that the distance between the molecules of interest in the zeolite L channels is in general large enough so that Equations (1) and (2) are good approximations. We illustrate this for DMPOPOP (Figure 5), for which we calculate
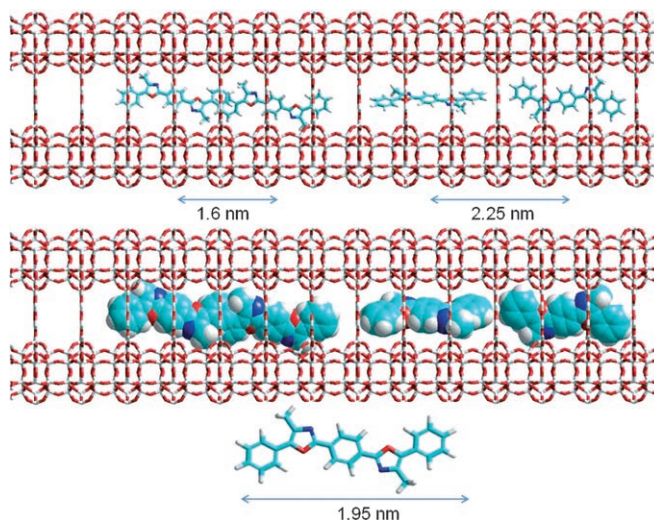

Figure 5. DMPOPOP in the channels of zeolite L. Two situations are compared: A molecule occupying three unit cells, leading to a centre-to-centre distance of 2.25 nm (right), and two molecules squeezed together resulting in a distance of 1.6 nm so that the J-aggregate coupling β_c is no longer negligible (left).

the length of the ETDM to be about 0.17 nm, while the length of the molecule is 1.95 nm. The figure also illustrates that there might be space enough for the phenyl groups at both ends of the molecule to overlap to some extent so that the J-aggregate coupling strength β_c from Equation (2) is not negligible, whereas in the case of PR149 the distance becomes so large that the level splitting is expected to be small and probably negligible.

Applications

An antenna material that absorbs all light in a specific wavelength range and transfers the electronic excitation energy by means of FRET to well-organised acceptors offers a unique possibility for developing dye-sensitised solar cells, luminescent solar concentrators (LSC) or colour-changing media. A dye–zeolite-sensitised solar cell functions by first absorbing light over a broad spectral range. The excitation energy then migrates radiationlessly among the inserted dyes towards the stopcock molecules. From there, FRET to the semiconductor takes place across a very thin insulating layer. The injected electronic excitation energy can now be used for driving the charge-separation process in the active medium. Finally, the resulting electrical current is collected through appropriate contacts. A more detailed report of this

concept is given in reference [23]. Here we discuss a new approach for solving an old problem of LSC. A LSC is a transparent plate containing luminescent chromophores.[24] Light enters the face of the plate and is absorbed and ree-mitted by these centres. A fraction of the luminescent light is trapped by total internal reflection and guided to the edges of the plate, at which it can be converted to electricity by a photovoltaic device. As the edge area of the plate is much smaller than the face area, the LSC operates as a concentrator of light. A major drawback in conventional LSC is the overlap between absorption and emission spectra, which is, as a basic principle, considerable in strongly luminescent molecules. Self-absorption therefore becomes an important loss mechanism. As a solution to this problem, antenna materials as explained in Figure 3 can be used. Absorption and emission spectra are separated by employing an absorbing dye present in large excess and a monolayer of an emitting dye, both in the zeolite channels.[25] A further advantage of using such a material is that the photostability of many dyes can be considerably improved by including them into the channels of zeolite L. The photophysical and photochemical behaviour of the molecules depend on the loading, the co-cations and the solvent present in the channels. The influence of the proton activity in the channels of zeolite L has been discussed recently.[22] The influence of the co-cations is especially important in absence of any solvent. Under such conditions a pronounced heavy atom effect can lead to very high phosphorescence yields.[26] Here, we report data of fully hydrated dye–zeolite L materials, implying that each unit cell contains water molecules. Figure 6 illustrates an experiment in which PC21$^+$ was used as absorbing dye and Ox$^+$ as emitter. The ratio between the donor and the emitter is about 15:2 in this experiment and the thickness of the active layer, which is embedded between two glass plates, is in the order of a few micrometers. Light scattering was suppressed by a procedure reported in reference [27].

Figure 6. Luminescent solar concentrator (LSC). A) LSC based on oriented dye–zeolite crystals. The channels of the disc-shaped zeolite crystals run perpendicular to the face of the LSC. The schematic axial cut (right) shows the double cone distribution of the ETDM for two different dyes. The blue double cones represent the light-absorbing molecules (large cone angle), whereas the green double cones indicate the light-emitting molecules (small cone angle). The concentration of the latter is kept low to avoid self-absorption. The red cone illustrates an escape cone originating at a light-emitting molecule located close to a channel entrance. B) Small fluorescent concentrator (2×1 cm) with PC21$^+$ as donor and Ox$^+$ as acceptor (acting as emitter). Left: appearance of the device. Right: fluorescence under near UV illumination. C) Absorption (dotted) and fluorescence spectra (solid) of PC21$^+$ and Ox$^+$ in zeolite L. The spectral overlap between the fluorescence spectrum of the donor and the acceptor is shaded. D) Excitation (dotted) and fluorescence spectrum of the Ox$^+$,PC21$^+$-zeolite L material. The excitation spectrum was measured at 640 nm. The fluorescence spectrum was measured by excitation at 425 nm where Ox$^+$ does not absorb. Energy transfer from PC21$^+$ to Ox$^+$ is considerable.

Conclusions

The combination of a tuneable host morphology and the possibility of obtaining highly organised molecular patterns of guests leads to a variety of potential optical and photo-electronic applications of dye–zeolite L materials. Strongly absorbing systems exhibiting efficient energy transfer along the *c* axis of the zeolite crystals are accessible by inclusion of multiple types of dyes, forming the basis for novel light-harvesting devices. The energy-transfer processes can be fine-tuned by an appropriate choice of dye molecules, whereas the ordering of the dyes can be extended to the macroscopic level by an oriented arrangement of the dye-loaded zeolite crystals. The robust zeolite framework can further be selectively functionalised at the external crystal surfaces and/or the pore entrances. This versatility can be exploited to establish communication pathways by means of energy transfer. Finally, the embedding of dye-loaded zeolite crystals into orga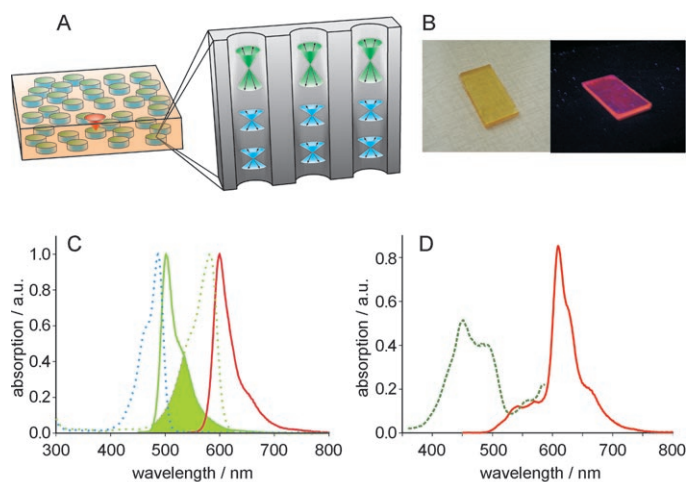nic matrices opens possibilities for the de-velopment of devices such as novel luminescent solar concentrators or sensitised solar cells.

[1] a) M. Ganschow, C. Hellriegel, E. Kneuper, M. Wark, C. Thiel, G. Schulz-Ekloff, C. Bräuchle, D. Wöhrle, *Adv. Funct. Mater.* **2004**, *14*, 269–276; b) C. Jung, C. Hellriegel, J. Michaelis, C. Bräuchle, D. Wöhrle, B. Platschek, T. Bein, *J. Am. Chem. Soc.* **2007**, *129*, 5570–5579; c) C. Seebacher, C. Hellriegel, C. Bräuchle, M. Ganschow, D. Wöhrle, *J. Phys. Chem. B* **2003**, *107*, 5445–5452.

[2] a) T. Bein, *Studies in Surface Science and Catalysis, Vol. 168: Introduction to Zeolite Science and Practive*, 3rd ed. (Eds.: J. Cejka, H. van Bekkum, A. Corma, F. Schüth), Elsevier, Amsterdam, **2007**, pp. 611–658; b) Y. Wang, H. Li, W. Zhang, B. Liu, *Mater. Lett.* **2008**,

62, 3167–3170; c) B. Bussemer, D. Munsel, H. Wünscher, G. J. Mohr, U. W. Grummt, *J. Phys. Chem. B* **2007**, *111*, 8–15; M. N. Chrétien, *Pure Appl. Chem.* **2007**, *79*, 1–20; d) K. B. Yoon, *Acc. Chem. Res.* **2007**, *40*, 29–40; e) S. Hashimoto, H. R. Moon, K. B. Yoon, *Microporous Mesoporous Mater.* **2007**, *101*, 10–18; f) S. Hashimoto, *J. Photochem. Photobiol. C* **2003**, *4*, 19–49; g) S. Hashimoto, M. Hagiri, N. Matsubara, S. Tobita, *Phys. Chem. Chem. Phys.* **2001**, *3*, 5043–5051.

[3] a) G. Calzaferri, M. Pauchard, H. Maas, S. Huber, A. Khatyr, T. Schaafsma, *J. Mater. Chem.* **2002**, *12*, 1–13; b) G. Calzaferri, S. Huber, H. Maas, C. Minkowski, *Angew. Chem.* **2003**, *115*, 3860–3888; *Angew. Chem. Int. Ed.* **2003**, *42*, 3732–3758; c) D. Brühwiler, G. Calzaferri, *Microporous Mesoporous Mater.* **2004**, *72*, 1–23; d) A. Devaux, K. Lutkouskaya, G. Calzaferri, L.-Q. Dieu, D. Brühwiler, L. De Cola, T. Torres, *Chimia* **2007**, *61*, 626–630; e) M. Busby, H. Kerschbaumer, G. Calzaferri, L. De Cola, *Adv. Mater.* **2008**, *20*, 1614–1618.

[4] G. Calzaferri, K. Lutkouskaya, *Photochem. Photobiol.*, in press, DOI: 10.1039/b804682b.

[5] a) D. W. Breck, *Zeolite Molecular Sieves*, Wiley, New York **1974**; b) S. Ernst, J. Weitkamp, *Catal. Today* **1994**, *19*, 27–60; c) Ch. Baerlocher, W. M. Meier, D. H. Olson, *Atlas of Zeolite Framework Types*, 5th ed., Elsevier, Amsterdam, **2001**; d) T. Ohsuna, B. Slater, F. Gao, J. Yu, Y. Sakamoto, G. Zhu, O. Terasaki, D. E. W. Vaughan, S. Qiu, C. R. A. Catlow, *Chem. Eur. J.* **2004**, *10*, 5031–5040; e) O. Larlus, V. P. Valtche, *Chem. Mater.* **2004**, *16*, 3381–3389.

[6] a) S. Megelski, G. Calzaferri, *Adv. Funct. Mater.* **2001**, *11*, 277–286; b) A. Zabala Ruiz, D. Brühwiler, T. Ban, G. Calzaferri, *Monatsh. Chem.* **2005**, *136*, 77–89; c) A. Zabala Ruiz, D. Brühwiler, L.-Q. Dieu, G. Calzaferri in *Materials Syntheses, a Practical Guide* (Eds.: U. Schubert, N. Hüsing, R. Laine), Springer, Wien, **2008**.

[7] N. Gfeller, G. Calzaferri, *J. Phys. Chem. B* **1997**, *101*, 1396–1408.

[8] a) T. Förster, *Ann. Phys.* **1948**, *437*, 55–75; b) V. May, O. Kühn, *Charge and Energy Transfer Dynamics in Molecular Systems*, 2nd ed., Wiley-VCH, **2004**; c) G. D. Scholes, C. Curutchet, B. Mennucci, R. Cammi, J. Tomasi, *J. Phys. Chem. B* **2007**, *111*, 6978–6982.

[9] C. Minkowski, G. Calzaferri, *Angew. Chem.* **2005**, *117*, 5459–5463; *Angew. Chem. Int. Ed.* **2005**, *44*, 5325–5329.

[10] a) A. Zabala Ruiz, H. Li, G. Calzaferri, *Angew. Chem.* **2006**, *118*, 5408–5413; *Angew. Chem. Int. Ed.* **2006**, *45*, 5282–5287; b) H. Li, Y. Wang, W. Zhang, B. Liu, G. Calzaferri, *Chem. Commun.* **2007**, 2853–2854; c) G. Calzaferri, A. Zabala Ruiz, H. Li, S. Huber, PCT/CH2006/000394; priority US 60/698,480 and CH 1266/05, **2005**.

[11] M. Pauchard, A. Devaux, G. Calzaferri, *Chem. Eur. J.* **2000**, *6*, 3456–3470.

[12] a) G. Calzaferri, US and EU patent, WO 02/36490 A1, prior. date **2000**; b) H. Maas, G. Calzaferri, *Angew. Chem.* **2002**, *114*, 2389–2392; *Angew. Chem. Int. Ed.* **2002**, *41*, 2284–2288.

[13] S. Huber, G. Calzaferri, *Angew. Chem.* **2004**, *116*, 6906–6910; *Angew. Chem. Int. Ed.* **2004**, *43*, 6738–6742.

[14] a) Z. Popović, M. Busby, S. Huber, G. Calzaferri, L. De Cola, *Angew. Chem.* **2007**, *119*, 9056–9060; *Angew. Chem. Int. Ed.* **2007**, *46*, 8898–8902; b) Z. Popović, M. Otter, G. Calzaferri, L. De Cola, *Angew. Chem.* **2007**, *119*, 6301–6304; *Angew. Chem. Int. Ed.* **2007**, *46*, 6188–6191.

[15] G. Calzaferri, H. Li, *Proc. SPIE* **2008**, *7002*, in press, DOI: 10.1117/12.787026.

[16] S. Megelski, A. Lieb, M. Pauchard, A. Drechsler, S. Glaus, C. Debus, A. J. Meixner, G. Calzaferri, *J. Phys. Chem. B* **2001**, *105*, 25–35.

[17] "The theory of molecular excitons": A. S. Davidov, *Sov. Phys. Usp.* **1964**, *82*, 145–178.

[18] a) "The molecular exciton model": E. G. McRae, M. Kasha in *Physical Progress in Radiation Biology*, Academic Press, New York, **1964**, pp. 23–42; b) T. Kobajashi, *J-Aggregates*, World Scientific, Singapore, **1996**.

[19] G. Calzaferri, H. Maas, M. Pauchard, M. Pfenniger, S. Megelski, A. Devaux, *Adv. Photochem.* **2002**, *27*, 1–50.

[20] M. Busby, C. Blum, M. Tibben, S. Fibikar, G. Calzaferri, V. Subramaniam, L. De Cola, *J. Am. Chem. Soc.*, DOI: 10.1021/ja801178p.

[21] a) R. Ziessel, C. Goze, G. Ulrich, M. Césario, P. Retailleau, A. Harriman, J. P. Rostron, *Chem. Eur. J.* **2005**, *11*, 7366–7378; b) G. Ulrich, R. Ziessel, A. Harriman, *Angew. Chem.* **2008**, *120*, 1202–1219; *Angew. Chem. Int. Ed.* **2008**, *47*, 1184–1201.

[22] R. Q. Albuquerque, G. Calzaferri, *Chem. Eur. J.* **2007**, *13*, 8938–8952.

[23] a) R. Koeppe, O. Bossart, G. Calzaferri, N. S. Sariciftci, *Sol. Energy Mater. Sol. Cells* **2007**, *91*, 986–995; b) G. Calzaferri, S. Huber, A. Devaux, A. Zabala Ruiz, H. Li, O. Bossart, L.-Q. Dieu, *Proc. SPIE* **2006**, *6192*, 619216-1–619216-11; c) L.-Q. Dieu, A. Devaux, I. López-Duarte, M. V. Martínez-Díaz, D. Brühwiler, G. Calzaferri, T. Torres, *Chem. Commun.* **2008**, 1187–1189.

[24] a) W. H. Weber, J. Lambe, *Appl. Opt.* **1976**, *15*, 2299–2300; b) A. Goetzberger, W. Greubel, *Appl. Phys.* **1977**, *14*, 123–139; c) J. S. Batchelder, A. H. Zewail, T. Cole, *Appl. Opt.* **1979**, *18*, 3090–3110; d) J. S. Batchelder, A. H. Zewail, T. Cole, *Appl. Opt.* **1981**, *20*, 3733–3754; e) P. Kittidachachan, L. Danos, T. J. J. Meyer, N. Alderman, T. Markvart, *Chimia* **2007**, *61*, 780–786.

[25] D. Brühwiler, L.-Q. Dieu, G. Calzaferri, *Chimia* **2007**, *61*, 820–822.

[26] a) V. Ramamurthy, J. V. Caspar, D. R. Corbin, *J. Phys. Chem.* **1990**, *94*, 3391–3393; b) V. Ramamurthy, J. V. Caspar, D. R. Corbin, D. E. Eaton, *J. Photochem. Photobiol. A* **1990**, *51*, 259–263; c) J. V. Caspar, V. Ramamurthy, D. R. Corbin, *Coord. Chem. Rev.* **1990**, *97*, 225–263; d) "Photoproceseses of organic molecules included in zeolites": V. Ramamurthy in *Photochemistry in Organised and Constrained Media* (Ed.: V. Ramamurthy), VCH, Weinheim, **1991**, pp. 429–493.

[27] S. Suárez, A. Devaux, J. Bañuelos, O. Bossart, A. Kunzmann, G. Calzaferri, *Adv. Funct. Mater.* **2007**, *17*, 2298–2306.